Coulomb Bound States of Strongly Interacting Photons

M. F. Maghrebi, M. J. Gullans, P. Bienias, S. Choi, I. Martin, O. Firstenberg, M. D. Lukin, H. P. Büchler, and A. V. Gorshkov

Phys. Rev. Lett. **115**, 123601 — Published 16 September 2015

DOI: 10.1103/PhysRevLett.115.123601

Coulomb bound states of strongly interacting photons

M. F. Maghrebi,[1,*] M. J. Gullans,[1,*] P. Bienias,[2] S. Choi,[3] I. Martin,[4]
O. Firstenberg,[5] M. D. Lukin,[3] H. P. Büchler,[2] and A. V. Gorshkov[1]

[1] *Joint Quantum Institute and Joint Center for Quantum Information and Computer Science, NIST/University of Maryland, College Park, Maryland 20742, USA*
[2] *Institute for Theoretical Physics III, University of Stuttgart, Germany*
[3] *Physics Department, Harvard University, Cambridge, Massachusetts 02138, USA*
[4] *Materials Science Division, Argonne National Laboratory, Argonne, Illinois 60439, USA*
[5] *Department of Physics of Complex Systems, Weizmann Institute of Science, Rehovot 76100, Israel*

We show that two photons coupled to Rydberg states via electromagnetically induced transparency can interact via an effective Coulomb potential. This interaction gives rise to a continuum of two-body bound states. Within the continuum, metastable bound states are distinguished in analogy with quasi-bound states tunneling through a potential barrier. We find multiple branches of metastable bound states whose energy spectrum is governed by the Coulomb potential, thus obtaining a photonic analogue of the hydrogen atom. Under certain conditions, the wavefunction resembles that of a diatomic molecule in which the two polaritons are separated by a finite "bond length." These states propagate with a negative group velocity in the medium, allowing for a simple preparation and detection scheme, before they slowly decay to pairs of bound Rydberg atoms.

PACS numbers: 42.50.Nn, 32.80.Ee, 34.20.Cf, 42.50.Gy

Photons are fundamental massless particles which are essentially non-interacting for optical frequencies. However, a medium that couples light to its atomic constituents can induce interactions between photons. This interaction may lead to exotic, many-body states of light [1–3], or can be used as a basis for realizing deterministic quantum gates between two photons [4–7]. A promising approach to create strongly interacting photons is to couple the light to atomic Rydberg states [3, 4, 6, 8–36], as realized in recent experiments [37–52].

Rydberg polaritons are superpositions of Rydberg atoms and light, which propagate almost without dissipation under the conditions of electromagnetically induced transparency (EIT) [8, 53–55]. EIT strongly reduces the group velocity and makes Rydberg polaritons dispersive. The large admixture of the Rydberg state can induce strong interactions between polaritons via the inherent Rydberg-Rydberg interactions. Specifically, the blockade effect prevents the formation of two Rydberg polaritons within the so-called "blockade radius" of each other [38, 43, 48, 56–59]. When the probe photons are detuned from the atomic transition, they can form bound states. A shallow bound state of light was observed in recent experiments [45], while stronger interactions result in deep bound states of Rydberg polaritons tied together within the blockaded region [29]. One can imagine these bound states as consisting of a photon trapped by a Rydberg excitation in a deep square well.

In this Letter, we predict and explore a class of photonic states resembling diatomic molecular states in which the two bound photons can be separated by a nonzero "bond length." This is achieved by considering Rydberg polaritons with the quantized light red-detuned from the excited atomic state. In such a system, we show the existence of metastable bound states exhibiting the Coulomb spectrum, akin to the hydrogen atom. Such states can potentially be used as building blocks for more complex quantum states of light.

To gain an intuitive understanding, consider the level structure of the Rydberg medium shown in Fig. 1(a). The probe field coupling the ground state $|g\rangle$ to the intermediate excited state $|e\rangle$ is red-detuned by $\Delta > 0$, and the Rabi frequency of the control field coupling $|e\rangle$ to the Rydberg state $|r\rangle$ is Ω. For $\Omega \ll \Delta$, the Rydberg state is

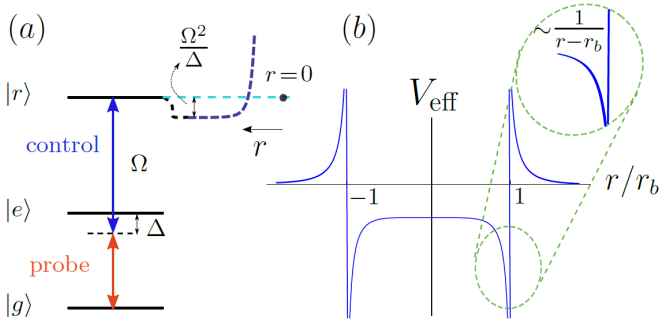

Figure 1: (a) The probe field couples the ground state $|g\rangle$ to the excited state $|e\rangle$ and is red-detuned by Δ. A control field with Rabi frequency Ω couples $|e\rangle$ to the Rydberg state $|r\rangle$ and is blue-detuned by Δ, thus putting the probe on an EIT transmission resonance. The Rydberg state is thus shifted downward by Ω^2/Δ. The van der Waals interaction with another reference Rydberg excitation at $r = 0$ can bring $|r\rangle$ into an absorption resonance with the two-photon transition. (b) The effective potential of two Rydberg polaritons as a function of their separation r exhibits a singularity at $|r| = r_b$ (the blockade radius) and behaves near this singularity as a Coulomb potential.

shifted downward by Ω^2/Δ [see Fig. 1(a)]. The van der Waals interaction $V(r) = C_6/r^6$ between Rydberg states modifies this picture (we assume $C_6 > 0$ or more generally $C_6\Delta > 0$). In particular, at small separations r, the strong interaction shifts two Rydberg states upward and out of resonance, while at large separations, the interaction is negligible and the energy level of each atom asymptotes to $-\Omega^2/\Delta$ (we set $\hbar = 1$). For intermediate separations on the order of the blockade radius r_b, defined by $V(r_b) = 2\Omega^2/\Delta$ [65], the system goes through a resonance (the factor of two arises since both atoms experience the Ω^2/Δ shift). This resonance, associated with a pair (or "molecule") of Rydberg atoms, endows the effective interaction $V_{\rm eff}(r)$ between two Rydberg polaritons with a singularity separating repulsion outside the blockade region from attraction inside; see Fig. 1(b). This effective interaction between two Rydberg polaritons can be roughly thought of as the difference in susceptibility of a single Rydberg polariton with and without a Rydberg excitation at $r = 0$ [45]. Interestingly, the effective potential near the resonant edge is that of the Coulomb interaction that changes sign across the blockade radius. This potential admits a continuum of states consisting of pairs of bound Rydberg atoms (Rydberg molecules) dressed by the photons. Within the continuum, we identify multiple branches of metastable states whose lifetime diverges with the strength of the interaction. When the effective energy of the two-polariton state lies below both $V_{\rm eff}(\infty)$ and $V_{\rm eff}(0)$, the bound state experiences a repulsive core and the wavefunction becomes double peaked near $\pm r_b$, resembling a diatomic molecular state. We further show that the group velocity of these states is negative, consistent with the fact that they have a finite lifetime.

Model.—To describe a propagating polariton in a Rydberg medium, we define $\mathcal{E}^\dagger(z)$ and $S^\dagger(z)$ as bosonic creation operators for a photon and a Rydberg excitation, respectively, at position z. They obey equal-time commutation relations $\left[\mathcal{E}(z), \mathcal{E}^\dagger(z')\right] = \left[S(z), S^\dagger(z')\right] = \delta(z - z')$. We define g to be the collectively enhanced atom-photon coupling [53] and assume that the decay rates 2γ of the excited state (satisfying $\gamma \ll \Delta$) and $2\gamma'$ of the Rydberg state can be neglected. In the regime of slow light ($g \gg \Omega$) and with large single-photon detuning ($\Delta \gg \Omega$), one can adiabatically eliminate the excited state $|e\rangle$ [29, 45]. The two-state Hamiltonian of the Rydberg medium is then

$$H = \int dz \begin{pmatrix} \mathcal{E} \\ S \end{pmatrix}^\dagger \begin{pmatrix} -ic\partial_z + g^2/\Delta & \Omega g/\Delta \\ \Omega g/\Delta & \Omega^2/\Delta \end{pmatrix} \begin{pmatrix} \mathcal{E} \\ S \end{pmatrix} + \frac{1}{2}\int dz\, dz' V(z - z') S^\dagger(z) S^\dagger(z') S(z') S(z). \quad (1)$$

In the Supplemental Material [60], we show that this treatment of the medium as a one-dimensional continuum of stationary atoms is experimentally relevant. In the absence of interactions, H diagonalizes into dark- and bright-state polaritons, where, at low energies, the former ($\propto gS^\dagger - \Omega\mathcal{E}^\dagger$ when $\partial_z = 0$) is mostly composed of $|r\rangle$ and travels at a reduced group velocity [53]. In the presence of interactions, the Hamiltonian in Eq. (1) can be projected onto the sector containing two-particles (at positions z and z') described by the quantum state $|\Phi\rangle$ with two-photon amplitude $EE(z, z')$, atom-photon amplitudes $ES(z, z')$ and $SE(z, z')$, and two-atom amplitude $SS(z, z')$. These are defined as $EE(z, z') = \langle 0|\mathcal{E}(z)\mathcal{E}(z')|\Phi\rangle$, $ES(z, z') = \langle 0|\mathcal{E}(z)S(z')|\Phi\rangle$, $SE(z, z') = \langle 0|S(z)\mathcal{E}(z')|\Phi\rangle$, and $SS(z, z') = \langle 0|S(z)S(z')|\Phi\rangle$, where $|0\rangle$ is the vacuum state. The problem is simplified by noting that, for two particles, the total energy ω and the center of mass momentum K are good quantum numbers.

In the limit $g \to 0$, the SS component decouples from the photonic amplitudes [$\omega SS(z, z') = (-2\Omega^2/\Delta + V(z-z'))SS(z-z')$] giving rise to a continuum of (delta-function) states of Rydberg molecules. Upon increasing g the continuum of states is still present while the wavefunction remains localized to the blockade radius. To see this, note that the Heisenberg equations of motion for the above amplitudes immediately lead [29, 60] to the Shrödinger-like equation

$$\left[-\frac{1}{m}\partial_r^2 + \frac{C_6}{r^6 - [r_b(\omega)]^6 + i0^+}\right]\psi(r) = E\psi(r), \quad (2)$$

where r is the relative coordinate of the two particles, and ψ is the symmetrized light-Rydberg wavefunction $\psi(r) \equiv [ES(r) + SE(r)]/2$. Notice that the van der Waals potential is replaced by an effective potential $V_{\rm eff}(r) = C_6/(r^6 - [r_b(\omega)]^6 + i0^+)$ modified within the blockaded region as in Fig. 1(b). (In contrast, for $C_6\Delta < 0$, the effective potential is a simple well $V_{\rm eff}(r) \propto -1/(r^6 + [r_b(\omega)]^6)$ of width $\sim 2r_b$ with no repulsive core at $r = 0$; this potential harbors bound states of width $\gtrsim r_b$ centered at $r = 0$, as studied in Ref. [29] and observed in Ref. [45].) For a nonzero ω, the blockade radius $r_b(\omega)$ depends on frequency via the resonant condition $C_6/[r_b(\omega)]^6 = 2\Omega^2/\Delta + \omega$ (the dependence of r_b on ω will often be implicit below). $i0^+$ in $V_{\rm eff}$ is obtained in the limit of vanishingly small γ and γ', which is further required by causality. In the limit of small energy and momentum, m is the mass of a single dark-state polariton due to the curvature of linear susceptibility and is given by $m = g^4/2c^2\Omega^2\Delta$ [61, 62], while the energy is given by $E = \omega - v_g K$ with $v_g = (\Omega^2/g^2)c$ being the EIT group velocity. More generally, the parameters in Eq. (2) can be simply derived from single polariton physics: For two Rydberg dark-state polaritons with momenta k_1 and k_2 and dispersion $\omega_{1,2} = \omega(k_{1,2})$, the constraints $\omega_1 + \omega_2 = \omega$ and $k_1 + k_2 = K$ yield an expression for the relative momentum $p = \sqrt{mE}$ consistent with the full expressions for m and E [29, 60].

Coulomb states.—The effective potential $V_{\rm eff}$ diverges as $1/(r \pm r_b)$ near the blockade radius, like a Coulomb po-

tential. Across the singularity, the wavefunction ψ should be continuous, while its derivative does not have to be. The full wavefunction $\Psi_{\omega,K}(r) = (EE, ES, SE, SS)$ has various components which are related to ψ as [29, 45]

$$\begin{aligned} EE(r) &= -\frac{2g\Omega/\Delta}{2g^2/\Delta + \omega - cK}\psi(r), \\ ES(r) &= \left(1 - \frac{ic}{(g^2+\Omega^2)/\Delta + \omega - cK/2}\partial_r\right)\psi(r), \\ SS(r) &= \frac{2g\Omega}{\Delta C_6}\mathcal{P}\left[\frac{\psi(r)}{r^{-6} - r_b^{-6}}\right] + \alpha\,\delta\,(r \pm r_b), \end{aligned} \tag{3}$$

where, for states with $\psi(r_b) \neq 0$, the principal value symbol $\mathcal{P}$ removes the $1/[r \pm r_b(\omega)]$ singularity in SS near the blockade radius. The coefficient α of the delta-function is determined by the discontinuity in the derivative of ψ at the blockade radius [60].

We now notice that Eqs. (2,3) admit a special set of solutions, which are a superposition of a normalizable wavefunction vanishing for $|r| \geq r_b$ [$\psi(r_b) = 0$] and a delta function singularity in the SS component, but without the $1/[r \pm r_b(\omega)]$ singularity. Such states can be interpreted in analogy to a "leaky box" where a quasi-bound particle tunnels through a potential barrier: for the leaky box, a true eigenstate is a superposition of the metastable bound state and a plane wave, which is a *momentum* eigenstate selected from a continuum. Similarly, for the above special eigenstates [with $\psi(r \geq r_b) = 0$], the role of the continuum of eigenstates is played by the delta functions in SS, which are *position* eigenstates. When the delta function is removed, the other components of the wavefunction form a metastable bound state. Furthermore, in the limit of an infinitely strong interaction, i.e. $g \to \infty$, our special eigenstates lose their delta function component [60]. This is again analogous to the leaky box, where, in the limit of an infinitely tall barrier (i.e. the no-leak limit), one obtains exact eigenstates confined to the box and decoupled from the plane-wave component sitting outside the box. Henceforth, we call the metastable bound states above (without the delta function) Coulomb states, and study their spectrum and other properties in detail.

Figure 2(a) shows the energy spectrum of the exact eigenstates (i.e. with the delta function) underlying the Coulomb states. The exact solutions are depicted as solid lines, while the dashed lines show the energy spectrum derived from the WKB quantization condition [applied to the case $\psi(\pm r_b) = 0$]

$$\int_{r_0}^{r_b} p(r)\,dr = n\pi, \qquad n = 1, 2, \cdots \tag{4}$$

with $p(r) = \sqrt{m(E - V_{\rm eff}(r))}$ defined by Eq. (2), and $r_0 < r_b$ is the classical turning point near the origin [66]. Figure 2(a) demonstrates that the WKB quantization agrees with the full solution for values of K near $2g^2/c\Delta$.

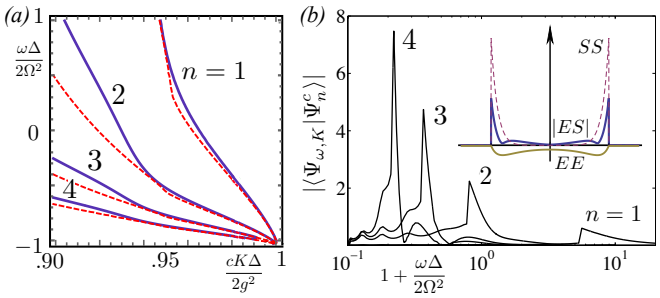

Figure 2: (a) Dispersion curves for the exact eigenstates underlying the metastable Coulomb bound states (only the first four branches n = 1-4 are shown) with $g^2 r_b/c\Delta = 40$ and $\Omega/g = 0.05$. The solid lines give the exact solution, while the dashed lines represent the WKB results. For $K \to 2g^2/c\Delta$, the WKB results are almost exact. The dispersion curves converge to one point with a negative slope, or group velocity. (b) Decomposition of the metastable Coulomb bound states (Ψ_n^c, defined as Ψ_{ω_n,K_n} with the delta-function contribution removed) into the continuum of exact eigenstates. Here we took $g^2 r_b/c\Delta = 40$ and $\Omega/g = 0.01$ with a fixed center of mass momentum $cK\Delta/2g^2 = 0.95$. The width of these distributions is much less than the energy spacing, indicating they are spectrally distinguishable. The inset shows the wavefunction components for the $n = 1$ Coulomb state with the parameters in (a) and $cK\Delta/2g^2 = 0.98$. (The EE component is exaggerated by a factor of 1.5 for better visibility.)

When K is close to $2g^2/c\Delta$, we can analytically compute the integral in Eq. (4) to find

$$\frac{1 + \omega\Delta/2\Omega^2}{1 - cK\Delta/2g^2} = \mathcal{A}\frac{\left[g^2 r_b(\omega)/c\Delta\right]^2}{n^2}, \tag{5}$$

where $\mathcal{A} = \left[\Gamma(2/3)/\Gamma(1/6)\sqrt{\pi}\right]^2 \approx 0.014$ and Γ is the gamma function. If r_b were independent of ω, Eq. (5) would imply that ω is quantized as $1/n^2$ (plus a constant), reminiscent of the energy spectrum of the Coulomb potential. However, due to the ω dependence of r_b, the quantization changes to $\omega_n \sim 1/n^{3/2}$ (plus a constant) [67], which still sharply contrasts with the finite-square-well energy quantization in Refs. [29, 45].

The fact that the blockade radius, and, thus, the interaction strength, is sensitive to frequency is a typical feature of nonlinear optical systems [13]. We also stress that $4g^2 r_b/c\Delta$ is identical to the figure of merit in the far-detuned regime $OD_b\gamma/\Delta$, where OD_b is the optical depth per blockade radius. The figure of merit quantifies the strength of the interaction as two polaritons imprint a phase $\sim OD_b\gamma/\Delta$ on each other [45].

With the dispersion in hand, we now explore the stability of the Coulomb states. The solutions given by Eq. (3) are a complete set of eigenstates for the two-particle Hilbert space. To normalize these states, we take K to be fixed and use the energy normalization $\langle\Psi_{\omega',K}|\Psi_{\omega,K}\rangle = \delta(\omega - \omega')$. We can then verify the metastability of the Coulomb states ($\psi[r_b(\omega)] = 0$) with

the delta-function removed by looking at their spectral width, i.e. their decomposition into the normalized eigenstates. Figure 2(b) shows this decomposition for several n, where we see that the Coulomb states are sharply peaked at the expected frequencies. The width of these distributions can be much narrower than the spacing between states, a strong signature of spectral distinguishability [63]. Furthermore, the Coulomb states converge to the exact eigenstates for a very strong interaction strength, which is analogous to the leaky box in the limit of an infinitely deep potential [60].

A unique feature of the dispersion curves in Fig. 2(a) is that their slope, and thus the group velocity, is negative. While true eigenstates cannot have a negative group velocity in the absence of left-moving modes (Supplemental Material [60]), Coulomb states are not exact eigenstates and eventually decay into Rydberg molecules. Equation (5) gives the group velocity as $v = -\mathcal{A}\left(g^2 r_b/c\Delta\right)^2 v_g/n^2$, where v_g is the EIT group velocity. Therefore, the velocity is also quantized as $1/n^2$ for different branches of bound states (and fixed values of ω). This quantization and the negative sign make the group velocity an ideal signature for detecting different Coulomb states and distinguishing them from the bound states of Refs. [29, 45]. We also remark that a small γ ($\ll \Delta$) contributes to the energy a small imaginary part, proportional to γ/Δ, which thus becomes negligible for large detuning.

We now show how to prepare these states and measure their dispersion. We assume that we have access to an additional hyperfine ground state $|q\rangle$, which, as shown in Fig. 3(a), is connected to both $|g\rangle$ and the Rydberg state $|r\rangle$ through two-photon transitions via an excited state $|e'\rangle$. With these additional states, we can effectively turn on and off the polariton interactions by applying a fast π-pulse on the two-photon transition between $|q\rangle$ and $|r\rangle$.

The preparation procedure is as follows. First, we store two identical photons (equivalently a weak coherent state followed by postselection) in the atomic state $|q\rangle$ using standard protocols [53, 64]. To have a significant overlap with the Coulomb states once we map to $|r\rangle$, the state has to have the correct center of mass momentum K. To achieve this, we introduce a linear energy gradient E' along the atomic cloud for a time τ, which could be achieved with a magnetic field gradient, another optical beam, or microwave field. This will impart a phase $e^{-iE'\tau R}$ on the stored two-photon state. By choosing the appropriate τ and then mapping $|q\rangle$ to $|r\rangle$, we can selectively excite different Coulomb states provided they have a large enough spatial overlap with the initial product state input. As the bound states travel with negative group velocity, the Coulomb state component will separate from the rest of the wavefunction. To detect the state, one can then map the Rydberg state back to $|q\rangle$

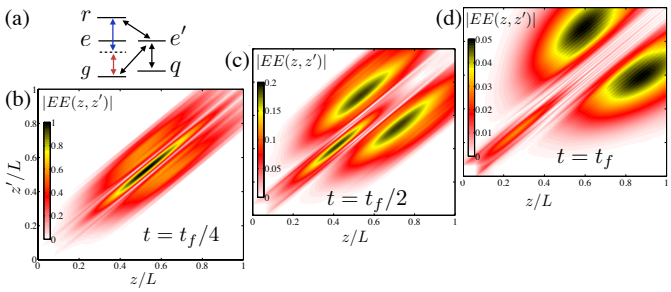

Figure 3: (a) Level structure used to prepare initial SS distribution. (b-d) Time evolution of a wavepacket with all components initially zero except SS, which is chosen to be a Gaussian wavepacket of variational $n = 1$ Coulomb state solutions (with the delta function removed) centered at $\omega = 0$ and having width $\Omega^2/2\Delta$ [60]. Specifically, $|EE|$, initially zero, is shown after the initial transient evolution subsides at (b) $t = t_f/4$, and at (c) $t = t_f/2$ and (d) $t = t_f$, where $t_f = 5.5\,\Delta/\Omega^2$. The wavepacket within the blockade radius has the expected shape of the Coulomb state, propagates backward, and decays, while the wavepacket outside the blockade radius propagates forward with v_g and disperses. We took a medium of length $L = 16\,r_b$, $g^2\,r_b/c\Delta = 5$, $g/2\pi = 17$ GHz, $\Omega/2\pi = 1.5$ MHz, $r_b = 25$ μm, $\Delta/2\pi = 30$ MHz, $\gamma/2\pi = 3$ MHz, and $\gamma'/2\pi = 5$ kHz [60].

and either measure the population of the state $|q\rangle$ directly or retrieve the state into light. In Fig. 3(b-d), for realistic parameters (including γ and γ') [41], we verify this approach by preparing a variational state that has a large overlap with the SS component of the Coulomb state [shown in Fig. 3(b)] with other components equal to zero and solve numerically for the time evolution [60]. In this case, the effective energy E of the bound state lies above $V_{\rm eff}(0)$ and the wavefunction is peaked at $r = 0$, similar to Refs. [29, 45]. We have also verified that, when $E < V_{\rm eff}(0)$, the backward propagating state becomes double peaked (in contrast to Refs. [29, 45]) and that, for smaller decay rates and larger $g^2\,r_b/c\Delta$, the negative group velocity observed in the numerics agrees with the WKB prediction from Eq. (4) for the $n = 1$, 2 and 3 Coulomb states within a few percent in each case [60].

Outlook.—While our proposal opens the avenue for the creation of Coulomb-like two-photon states, we expect that a wide class of both useful and exotic two-photon and multi-photon states can be created via refined engineering of photon-photon interactions, e.g. by using microwave fields [43]. The detailed understanding of the two-photon Rydberg-EIT physics provided by this work also opens up an avenue towards understanding the full—and much richer—many-body problem involving an arbitrary number of photons in any dimension.

We thank D. Chang, R. Qi, and Y. Wang for discussions. This work was supported by ARL, NSF PFC at the JQI, the NRC, NSF PIF, CUA, AFOSR, ARO, AFOSR MURI, Center for Integrated Quantum Sci-

ence and Technology (IQST), the Deutsche Forschungsgemeinschaft (DFG) within SFB TRR 21, the EU Marie Curie ITN COHERENCE, CUA, DARPA QUINESS, Packard Foundation, and the National Science Foundation. The work of IM was supported by the U.S. Department of Energy, Office of Science, Materials Sciences and Engineering Division.

---

* These two authors contributed equally.

[1] I. Carusotto and C. Ciuti, Rev. Mod. Phys. **85**, 299 (2013).

[2] D. E. Chang, V. Gritsev, G. Morigi, V. Vuletić, M. D. Lukin, and E. A. Demler, Nature Phys. **4**, 884 (2008).

[3] J. Otterbach, M. Moos, D. Muth, and M. Fleischhauer, Phys. Rev. Lett. **111**, 113001 (2013).

[4] I. Friedler, D. Petrosyan, M. Fleischhauer, and G. Kurizki, Phys. Rev. A **72**, 043803 (2005).

[5] E. Shahmoon, G. Kurizki, M. Fleischhauer, and D. Petrosyan, Phys. Rev. A **83**, 033806 (2011).

[6] A. V. Gorshkov, J. Otterbach, M. Fleischhauer, T. Pohl, and M. D. Lukin, Phys. Rev. Lett. **107**, 133602 (2011).

[7] D. Paredes-Barato and C. S. Adams, Phys. Rev. Lett. **112**, 040501 (2014).

[8] M. D. Lukin, M. Fleischhauer, R. Cote, L. M. Duan, D. Jaksch, J. I. Cirac, and P. Zoller, Phys. Rev. Lett. **87**, 037901 (2001).

[9] A. E. B. Nielsen and K. Mølmer, Phys. Rev. A **81**, 043822 (2010).

[10] B. Olmos and I. Lesanovsky, Phys. Rev. A **82**, 063404 (2010).

[11] T. Pohl, E. Demler, and M. D. Lukin, Phys. Rev. Lett. **104**, 043002 (2010).

[12] D. Petrosyan, J. Otterbach, and M. Fleischhauer, Phys. Rev. Lett. **107**, 213601 (2011).

[13] S. Sevinçli, N. Henkel, C. Ates, and T. Pohl, Phys. Rev. Let. **107**, 153001 (2011).

[14] J. Honer, R. Löw, H. Weimer, T. Pfau, and H. P. Büchler, Phys. Rev. Lett. **107**, 093601 (2011).

[15] M. Saffman and T. G. Walker, Phys. Rev. A **66**, 065403 (2002).

[16] L. H. Pedersen and K. Molmer, Phys. Rev. A **79**, 012320 (2009).

[17] J. D. Pritchard, C. S. Adams, and K. Mølmer, Phys. Rev. Lett. **108**, 043601 (2012).

[18] C. Guerlin, E. Brion, T. Esslinger, and K. Mølmer, Phys. Rev. A **82**, 053832 (2010).

[19] J. Stanojevic, V. Parigi, E. Bimbard, A. Ourjoumtsev, P. Pillet, and P. Grangier, Phys. Rev. A **86**, 021403 (2012).

[20] F. Bariani, Y. O. Dudin, T. A. B. Kennedy, and A. Kuzmich, Phys. Rev. Lett. **108**, 030501 (2012).

[21] F. Bariani, P. M. Goldbart, and T. A. B. Kennedy, Phys. Rev. A **86**, 041802 (2012).

[22] J. Stanojevic, V. Parigi, E. Bimbard, A. Ourjoumtsev, and P. Grangier, Phys. Rev. A **88**, 053845 (2013).

[23] M. M. Müller, A. Kölle, R. Löw, T. Pfau, T. Calarco, and S. Montangero, Phys. Rev. A **87**, 053412 (2013).

[24] J.-F. Huang, J.-Q. Liao, and C. P. Sun, Phys. Rev. A **87**, 023822 (2013).

[25] M. Gärttner and J. Evers, Phys. Rev. A **88**, 033417 (2013).

[26] G. W. Lin, J. Yang, X. M. Lin, Y. P. Niu, and S. Q. Gong, arXiv:1308.2782 (2013).

[27] A. V. Gorshkov, R. Nath, and T. Pohl, Phys. Rev. Lett. **110**, 153601 (2013).

[28] B. He, A. V. Sharypov, J. Sheng, C. Simon, and M. Xiao, Phys. Rev. Lett. **112**, 133606 (2014).

[29] P. Bienias, S. Choi, O. Firstenberg, M. F. Maghrebi, M. Gullans, M. D. Lukin, A. V. Gorshkov, and H. P. Büchler, Phys. Rev. A **90**, 053804 (2014).

[30] M. Gärttner, S. Whitlock, D. W. Schönleber, and J. Evers, Phys. Rev. A **89**, 063407 (2014).

[31] Y.-M. Liu, D. Yan, X.-D. Tian, C.-L. Cui, and J.-H. Wu, Phys. Rev. A **89**, 033839 (2014).

[32] A. Grankin, E. Brion, E. Bimbard, R. Boddeda, I. Usmani, A. Ourjoumtsev, and P. Grangier, New J. Phys. **16**, 043020 (2014).

[33] W. Li, D. Viscor, S. Hofferberth, and I. Lesanovsky, Phys. Rev. Lett. **112**, 243601 (2014).

[34] H. Wu, M.-M. Bian, L.-T. Shen, R.-X. Chen, Z.-B. Yang, and S.-B. Zheng, Phys. Rev. A **90**, 045801 (2014).

[35] G. W. Lin, J. Gong, J. Yang, Y. H. Qi, X. M. Lin, Y. P. Niu, and S. Q. Gong, Phys. Rev. A **89**, 043815 (2014).

[36] I. I. Beterov, T. Andrijauskas, D. B. Tretyakov, V. M. Entin, E. A. Yakshina, I. I. Ryabtsev, and S. Bergamini, Phys. Rev. A **90**, 043413 (2014).

[37] J. D. Pritchard, D. Maxwell, A. Gauguet, K. J. Weatherill, M. P. A. Jones, and C. S. Adams, Phys. Rev. Lett. **105**, 193603 (2010).

[38] Y. O. Dudin and A. Kuzmich, Science **336**, 887 (2012).

[39] Y. O. Dudin, F. Bariani, and A. Kuzmich, Phys. Rev. Lett. **109**, 133602 (2012).

[40] Y. O. Dudin, L. Li, F. Bariani, and A. Kuzmich, Nature Phys. **8**, 790 (2012).

[41] T. Peyronel, O. Firstenberg, Q.-Y. Liang, S. Hofferberth, A. V. Gorshkov, T. Pohl, M. D. Lukin, and V. Vuletic, Nature (London) **488**, 57 (2012).

[42] V. Parigi, E. Bimbard, J. Stanojevic, A. J. Hilliard, F. Nogrette, R. Tualle-Brouri, A. Ourjoumtsev, and P. Grangier, Phys. Rev. Lett. **109**, 233602 (2012).

[43] D. Maxwell, D. J. Szwer, D. Paredes-Barato, H. Busche, J. D. Pritchard, A. Gauguet, K. J. Weatherill, M. P. A. Jones, and C. S. Adams, Phys. Rev. Lett. **110**, 103001 (2013).

[44] C. S. Hofmann, G. Günter, H. Schempp, M. Robert-de Saint-Vincent, M. Gärttner, J. Evers, S. Whitlock, and M. Weidemüller, Phys. Rev. Lett. **110**, 203601 (2013).

[45] O. Firstenberg, T. Peyronel, Q.-Y. Liang, A. V. Gorshkov, M. D. Lukin, and V. Vuletic, Nature (London) **502**, 71 (2013).

[46] G. Günter, H. Schempp, M. Robert-de Saint-Vincent, V. Gavryusev, S. Helmrich, C. S. Hofmann, S. Whitlock, and M. Weidemüller, Science **342**, 954 (2013).

[47] H. Gorniaczyk, C. Tresp, J. Schmidt, H. Fedder, and S. Hofferberth, Phys. Rev. Lett. **113**, 053601 (2014).

[48] P. Schausz, M. Cheneau, M. Endres, T. Fukuhara, S. Hild, A. Omran, T. Pohl, C. Gross, S. Kuhr, and I. Bloch, Nature **491**, 87 (2012).

[49] S. Baur, D. Tiarks, G. Rempe, and S. Dürr, Phys. Rev. Lett. **112**, 073901 (2014).

[50] P. Schauß, J. Zeiher, T. Fukuhara, S. Hild, M. Cheneau, T. Macrì, T. Pohl, I. Bloch, and C. Gross, arXiv:1404.0980 (2014).

[51] D. Tiarks, S. Baur, K. Schneider, S. Dürr, and G. Rempe, Phys. Rev. Lett. **113**, 053602 (2014).

[52] D. Maxwell, D. J. Szwer, D. Paredes-Barato, H. Busche, J. D. Pritchard, A. Gauguet, M. P. A. Jones, and C. S. Adams, Phys. Rev. A **89**, 043827 (2014).

[53] M. Fleischhauer and M. D. Lukin, Phys. Rev. Lett. **84**, 5094 (2000).

[54] M. Fleischhauer, A. Imamoglu, and J. P. Marangos, Rev. Mod. Phys. **77**, 633 (2005).

[55] M. Saffman, T. G. Walker, and K. Mølmer, Rev. Mod. Phys. **82**, 2313 (2010).

[56] A. Gaetan, Y. Miroshnychenko, T. Wilk, A. Chotia, M. Viteau, D. Comparat, P. Pillet, A. Browaeys, and P. Grangier, Nature Phys. **5**, 115 (2013).

[57] E. Urban, T. A. Johnson, T. Henage, L. Isenhower, D. D. Yavuz, T. G. Walker, and M. Saffman, Nature Phys. **5**, 110 (2013).

[58] H. Schempp, G. Günter, M. Robert-de Saint-Vincent, C. S. Hofmann, D. Breyel, A. Komnik, D. W. Schönleber, M. Gärttner, J. Evers, S. Whitlock, et al., Phys. Rev. Lett. **112**, 013002 (2014).

[59] R. Heidemann, U. Raitzsch, V. Bendkowsky, B. Butscher, R. Löw, L. Santos, and T. Pfau, Phys. Rev. Lett. **99**, 163601 (2007).

[60] See Supplemental Material at http://link.aps.org/supplemental/??? for details omitted in the main text.

[61] F. E. Zimmer, A. André, M. D. Lukin, and M. Fleischhauer, Opt. Comm. **264**, 441 (2006).

[62] F. E. Zimmer, J. Otterbach, R. G. Unanyan, B. W. Shore, and M. Fleischhauer, Phys. Rev. A **77**, 063823 (2008).

[63] M. Razavy, *Quantum theory of tunneling* (World Scientific, 2003).

[64] A. V. Gorshkov, A. André, M. D. Lukin, and A. S. Sørensen, Phys. Rev. A **76**, 033804 (2007).

[65] For notational convenience, we deviate from Refs. [6, 45] and define $V(r_b) = 2\Omega^2/\Delta$ instead of $V(r_b) = \Omega^2/\Delta$.

[66] If no turning point exists, $r_0 = 0$, and the quantization condition changes to $n \to n - 1/4$.

[67] We recover $\omega_n \sim 1/n^2$ by rescaling ω and K by $2\Omega^2/\Delta$ and $2g^2/c\Delta$, respectively, and taking a line perpendicular to the dispersion curves near $K = 1$.